Biochemistry and Biophysics Reports 11 (2017) 174–181

Contents lists available at ScienceDirect

Biochemistry and Biophysics Reports

journal homepage: www.elsevier.com/locate/bbrep

Visualization of ceramide channels in lysosomes following endogenous palmitoyl-ceramide accumulation as an initial step in the induction of necrosis

Mototeru Yamane[a,*], Shota Moriya[a], Hiroko Kokuba[b]

[a] Department of Biochemistry, Tokyo Medical University, 6-1-1 Shinjuku, Shinjuku-ku, Tokyo 160, Japan
[b] Joint-Use Laboratories, Tokyo Medical University, 6-1-1 Shinjuku, Shinjuku-ku, Tokyo 160, Japan

ABSTRACT

In this study, we showed that the dual addition of glucosyl ceramide synthase and ceramidase inhibitors to A549 cell culture led to the possibility of ceramide channel formation via endogenous palmitoyl-ceramide accumulation with an increase in cholesterol contents in the lysosome membrane as an initial step prior to initiation of necrotic cell death. In addition, the dual addition led to black circular structures of 10–20 nm, interpreted as stain-filled cylindrical channels on transmission electron microscopy. The formation of palmitoyl-ceramide channels in the lysosome membrane causes the liberation of cathepsin B from lysosomes for necrotic cell death. On the other hand, necrotic cell death in the dual addition was not caused by oxidative stress or cathepsin B activity, and the cell death was free from the contribution of the translation of Bax protein to the lysosome membrane.

1. Introduction

In recent years, the formation of ceramide (Cer) channels that initiated apoptosis on their own or via interaction with BCL2-associated X protein (Bax) in the outer mitochondrial membrane, followed by the release of cytochrome c was firmly established [1–3]. On the other hand, direct interaction of mitochondrial Cer with the autophagosomal membrane bound-microtubule-associated protein 1 light chain 3B (LC3B)-II for mitophagy has been reported [4]. However, the functions of endogenous Cer accumulation in necrotic cell death remain unknown. The aim of this study was to clarify the relationship between endogenous palmitoyl-Cer (C16:0-Cer) accumulation with inhibition of the conversion pathway of Cer and concomitant necrotic cell death.

In A549 cells, active caspase 3 expression with C16:0-Cer accumulation in mitochondria was not detected by the blocking effect in the caspase 9 to caspase 3 process by survivin having an inhibitory effect on the activation of caspase 9 [5,6]. Therefore, endogenous C16:0-Cer accumulation in A549 cells would likely be related to a pathway (e.g., the pathway of necrotic cell death) distinct from the mitochondrial caspase-dependent pathway. Previously, we showed that a high concentration of DL-threo-1-phenyl-2-decanoylamino-3-morpholino-1-propanol [DL-PDMP, an inhibitor of glucosyl(Glc)-Cer synthase] in A549 cell culture caused massive autophagy with endoplasmic reticulum stress and endogenous C16:0-Cer accumulation via Cer synthase (CerS) 5 protein expression in A549 cells, followed by autophagic cell death 24 h after treatment [6]. Furthermore, we showed that the dual addition of DL-PDMP and N-[(1R,2R)-2-hydroxy-1-(hydroxy-methyl)-2-(4-nitrophenyl)ethyl]tetradecanamide (D-NMAPPD, an inhibitor of ceramidase) to A549 cell culture induced additional endogenous C16:0-Cer accumulation with CerS5 expression and necrotic cell death with lysosomal rupture along with the leakage of cathepsin B/alkalization 2–3 h afterwards [7]. If C16:0-Cer channels were formed in the lysosome membrane with endogenous C16:0-Cer accumulation via the activation of CerS5 and the inhibition of lysosomal acid ceramidase by D-

Abbreviations: Cer, ceramide; Bax, BCL2-associated X protein; LC3B, autophagosomal membrane bound-microtubule-associated protein 1 light chain 3B; C16:0-Cer, palmitoyl-Cer; DL-PDMP, DL-threo-1-phenyl-2-decanoylamino-3-morpholino-1-propanol; CerS, ceramide synthase; GlcCer, glucosyl ceramide; D-NMAPPD, N-[(1R,2R)-2-hydroxy-1-(hydroxy-methyl)-2-(4-nitrophenyl)ethyl]tetradecanamide; [D_7]d18:0, D-erythro-sphinganine-D_7; [D_7]d18:1, D-erythro-sphingosine-D_7; d18:1-[D_{31}]C16:0-Cer, N-palmitoyl [D_{31}]-D-erythro-sphingosine; ISs, internal standards; CA-74Me, [(2S,3S)-3-Propylcarbamoyloxirane-2-carbonyl]-L-isoleucyl-L-proline methyl ester; NAC, N-acetyl-L-cysteine; acridine orange, 3,6-Bis(dimethylamino) acridine hydrochloride; LAMP-2, lysosome-associated membrane protein 2; DMEM, Dulbecco's modified Eagle's medium; FBS, fetal bovine serum; PBS, phosphate buffered saline; DTT, dithiothreitol; SDS-PAGE, sodium dodecyl sulfate-polyacrylamide gel electrophoresis; ECL, enhanced chemiluminescence reagent; APCI, atmospheric pressure chemical ionization; MS, mass spectrometry; d18:0, sphinganine; d18:1, sphingosine; SIM, selected ion monitoring; DMSO, dimethyl sulfoxide; DAPI, 4′,6-diamidino-2-phenylindole; LMP, lysosomal membrane permeability

* Corresponding author.
E-mail addresses: cbc01664@nifty.com (M. Yamane), moriya@tokyo-med.ac.jp (S. Moriya), kokuba@tokyo-med.ac.jp (H. Kokuba).

http://dx.doi.org/10.1016/j.bbrep.2017.02.010
Received 24 November 2016; Received in revised form 7 February 2017; Accepted 27 February 2017
Available online 13 March 2017

NMAPPD, this possibility would be of interest as a function of the liberation of cathepsin B from lysosomes causing necrotic cell death via C16:0-Cer channels in the lysosome membrane distinct from the mitochondrial caspase-dependent pathway of apoptosis.

2. Materials and methods

2.1. Materials

D-*erythro*-sphinganine-D_7 ([D_7]d18:0), D-*erythro*-sphingosine-D_7 ([D_7]d18:1), and N-palmitoyl [D_{31}]-D-*erythro*-sphingosine (d18:1-[D_{31}]C16:0-Cer) as internal standards (ISs) labeled with stable isotopes were obtained from Avanti Polar Lipids, Inc. (Alabaster, AL). [(2S,3S)-3-propylcarbamoyloxirane-2-carbonyl]-L-isoleucyl-L-proline methyl ester (CA-074Me as an inhibitor of cathepsin B), N-acetyl-L-cysteine (NAC as an inhibitor of oxidative stress), 3,6-Bis(dimethylamino) acridine hydrochloride (acridine orange) solution (1 mg/mL water), 10% ammonia aqueous solution, cholesterol, dithiothreitol, and lithium dodecyl sulfate were purchased from Wako (Osaka, Japan). D-NMAPPD as an inhibitor of ceramidase was purchased from Cayman Chemical (Ann Arbor, MI). DL-PDMP was obtained from Biomol Research Laboratories (Plymouth Meeting, PA). β-cholestanol was obtained from Tokyo Chemical Industry Co., Ltd. (Tokyo, Japan).

2.2. A549 cell culture, induction of Cer accumulation

A549 cells (human lung adenocarcinoma cell line) were grown in humidified air with 5% CO_2 in Dulbecco's modified Eagle's medium (DMEM) (including 8.5 μM free fatty acids) prepared from Sigma D5796 including 400 μM L-serine, containing fetal bovine serum (FBS) at a concentration of 10% (v/v), at 37 °C. The induction of Cer accumulation was usually initiated 1 day after subculture below 90% confluence. Overgrown cells were unsuitable for obtaining the desired effects.

For the induction of Cer accumulation, 200 μM DL-PDMP and 65 μM D-NMAPPD in the culture medium were incubated for 2–5 h. For the inhibition of cathepsin B or oxidative stress, 20 μM CA-074Me or 5000 μM NAC was added to the culture medium.

2.3. Isolation of the lysosome-rich fraction from A549 cells

A549 cells were collected after incubation for 2 h by scraping with the culture medium and rinsing two times with Hank's balanced salt solution. Isolation of the lysosome-rich fraction from A549 cells was performed with Lysosome Enrichment Kit for Tissue and Cultured Cells (Thermo Scientific, Rockford, IL). After A549 cells had been added to 250 μM of Lysosome Enrichment Reagent A, the mixture was mixed by Vortex for 5 s, incubated on ice for 2 min, and treated by mild sonication (6–9 W of power) for 10 s. The suspension was mixed with 250 μM of Lysosome Enrichment Reagent B and centrifuged at 500 × *g* for 10 min at 4 °C. The supernatant was overlayed on the top of a prepared discontinuous density gradient and gradient centrifuged at 145,000 × *g* for 2 h at 4 °C. The lysosome-rich band was mixed with five volumes of phosphate buffered saline (PBS) and rinsed by centrifugation at 18,000 × *g* for 30 min. The residue was rinsed with PBS in a similar manner.

2.4. Western blotting with LAMP-2/Bax/β-actin antibodies

A549 cells were incubated for 2 h, scraped with the culture medium and rinsed two times with Hank's balanced salt solution. The cells or the suspension of the lysosome-rich fraction in 1.0 mL of 0.85% sodium chloride was mixed with 100 μL of 100% (1.0g/mL aqueous solution) trichloroacetic acid solution and left for 30 min at 0 °C. The mixture was centrifuged at 1500 × *g* for 5 min. The pellet was mixed with 80 μL of 9 M urea/2% Triton X100/1% dithiothreitol (DTT) and the mixture was treated with ultrasonic waves for 30 s. The mixture was mixed with 20 μL of 10% lithium dodecyl sulfate and made basic with 1 M Tris under ultrasonic waves for 30 s.

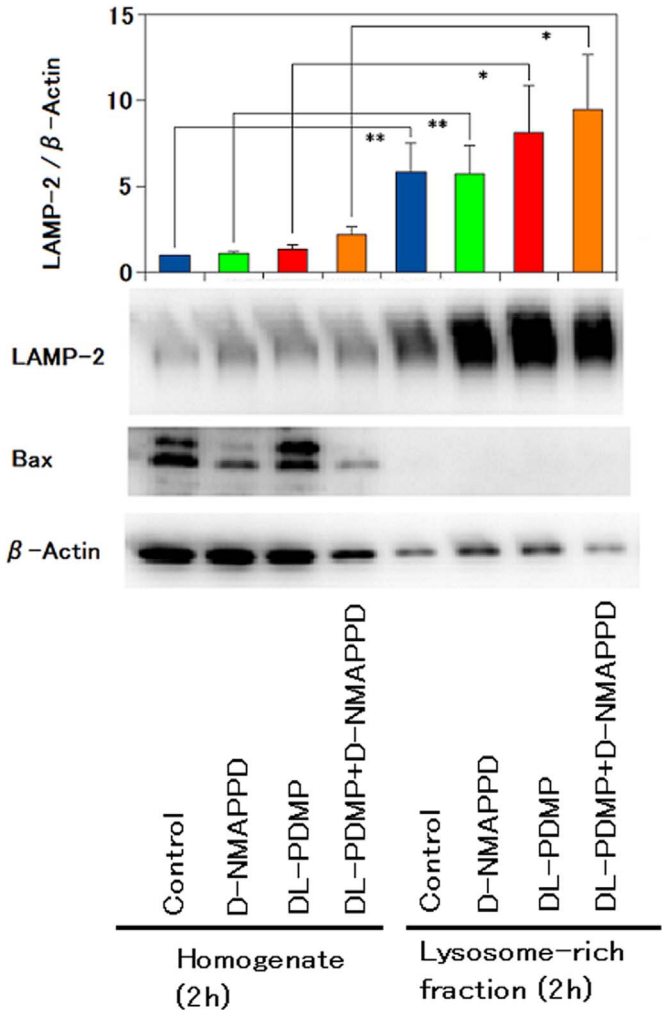

Fig. 1. The analysis of LAMP-2, Bax, and β-actin in the homogenate or lysosome-rich fraction from A549 cells by Western blotting. Western blotting analysis was achieved as described in Methods. LAMP-2/β-actin was high in the lysosome-rich fraction and LAMP-2 protein was concentrated in the lysosome-rich fraction. However, Bax protein was not detected in the lysosome-rich fraction. Data are presented as the mean values ± S.D. of three independent experiments;*P < 0.05 and **P < 0.01 as compared with the control or the individual addition.

Equal amounts of proteins were loaded onto the gels, separated by 15% sodium dodecyl sulfate polyacrylamide gel electrophoresis (SDS-PAGE), and transferred onto Immobilon-P membrane (Millipore, Billerica, MA). The membranes were probed with primary antibodies such as anti-LAMP-2 (clone H4B4; 1/1000 dilution) antibody, anti-BAX (clone N-20; 1/1000 dilution) antibody, and anti-β-actin (clone C4; 1/1000 dilution) antibody (all from Santa Cruz Biotechnology, Inc., Santa Cruz, CA) for 16 h at 4 °C. Immunoreactive proteins were detected with horseradish peroxidase-conjugated second antibody (Jackson, West Grove, PA; 1:25000 dilution) for 1 h at room temperature and an enhanced chemiluminescence reagent (ECL) (Millipore). Densitometry was performed using a Molecular Imager, ChemiDoc XRS System (Bio-Rad, Richmond, CA).

2.5. Lipid extraction of from A549 cells or the lysosome-rich fraction after various additions

A549 cells were collected each time by scraping with the culture medium and rinsing two times with Hank's balanced salt solution. Cells

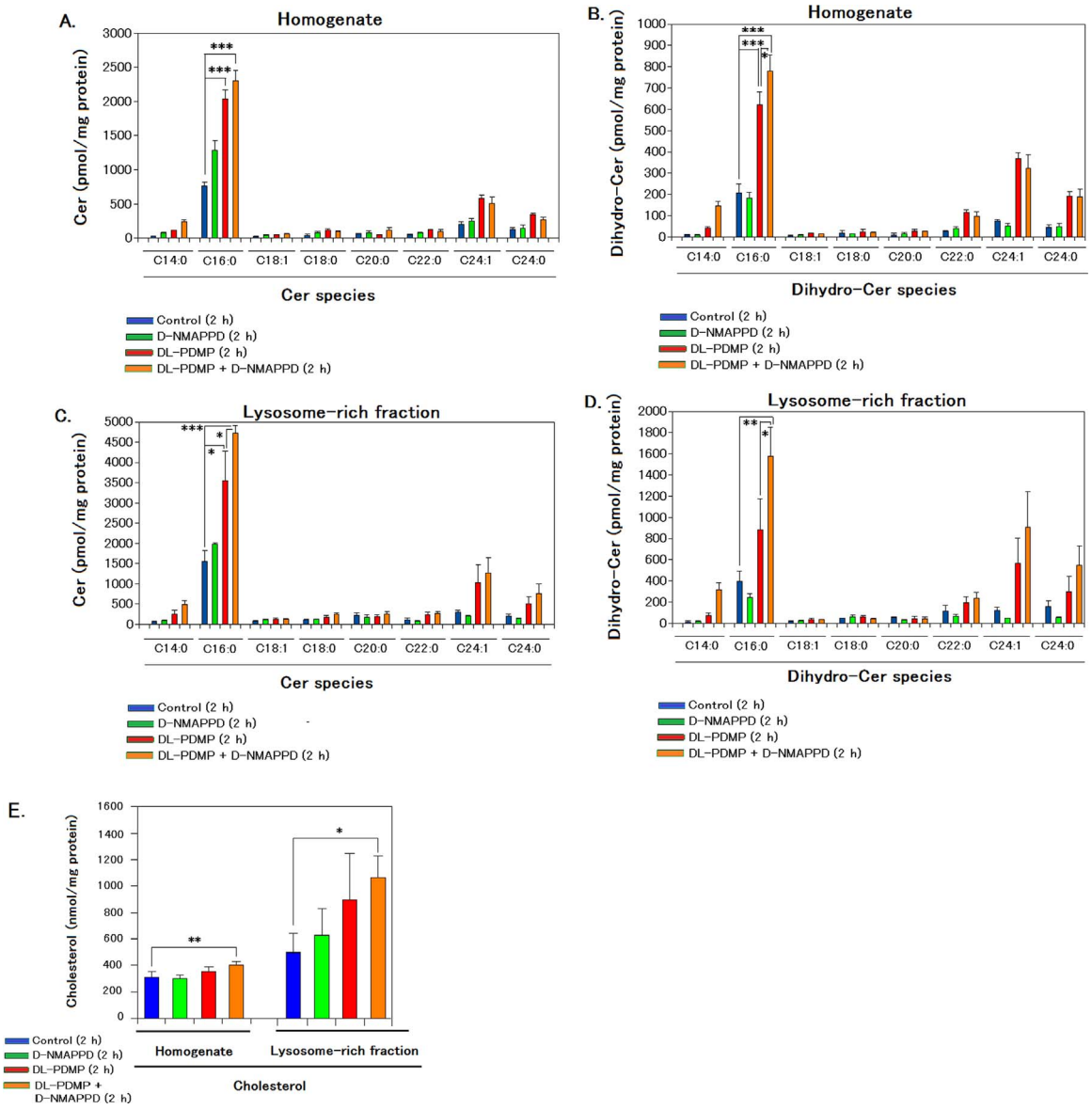

Fig. 2. The dual addition of DL-PDMP and D-NMAPPD caused an additional increase in C16:0-Cer, dihydro-C16:0-Cer or cholesterol contents in the lysosome-rich fraction of A549 cells 2 h afterwards, compared with the control or individual addition. The induction of Cer accumulation and extraction/analysis of Cers/dihydro-Cer/cholesterol in the homogenate or the lysosome-rich fraction were achieved as described in Methods. **A-D**, levels of Cer and dihydro-Cer species in the homogenate or the lysosomal rich fraction of A549 cells 2 h after the individual or dual addition. **E,** levels of cholesterol in the homogenate or the lysosome-rich fraction of A549 cells 2 h after the individual or dual addition. Data are presented as the mean values ± S.D. of three independent experiments; *P < 0.05, **P < 0.01, and ***P < 0.001 as compared with the control.

were homogenized for 30 s using a Polytron (Kinematica, Luzern, Switzerland) in 2.5 mL of 50 mM Tris-HCl buffer (pH 7.5). The protein concentration of the homogenate or the suspension of the lysosome-rich fraction was measured using BCA Protein Assay Reagents (Thermo Scientific). Extraction of Cers and dihydro-Cers in the homogenate or the suspension from the lysosome-rich fraction were performed using d18:1-[D_{31}]C16:0-Cer as the IS as described previously [7]. The extract was examined using an HPLC- atmospheric pressure chemical ionization (APCI)-mass spectrometry (MS) system.

Extraction of sphinganine (d18:0) and sphingosine (d18:1) in the homogenate described above or the suspension of the lysosome-rich fraction were performed using [D_7]d18:0 or [D_7]d18:1 as the IS as described previously [7]. The extract was examined using an HPLC-APCI-MS system.

2.6. Cholesterol contents in the suspension of the lysosome-rich fraction after various additions

To 1.0 mL of the homogenate described above or the suspension of the lysosome-rich fraction, 3.2 nmol of β-cholestanol as the IS, 2.0 mL of methanol, 1.0 mL of water, and 2.0 mL of chloroform were added, and the mixture was shaken for 30 s. The mixture was centrifuged at 600 × *g* for 10 min. Then, the lower layer was transferred to a glass tube. The collected chloroform solution was evaporated to dryness under reduced pressure. Afterwards, the residue was dissolved in 1.0 mL of chloroform: methanol (2:1) and 5-μL aliquots were examined using an HPLC-APCI-MS system.

2.7. HPLC-APCI-MS

To determine the d18:0, d18:1, Cer or dihydro-Cer content, HPLC-MS was performed using a Shimadzu (Kyoto, Japan) LCMS-2010EV mounted on an APCI probe, a quadrupole mass spectrometer, and

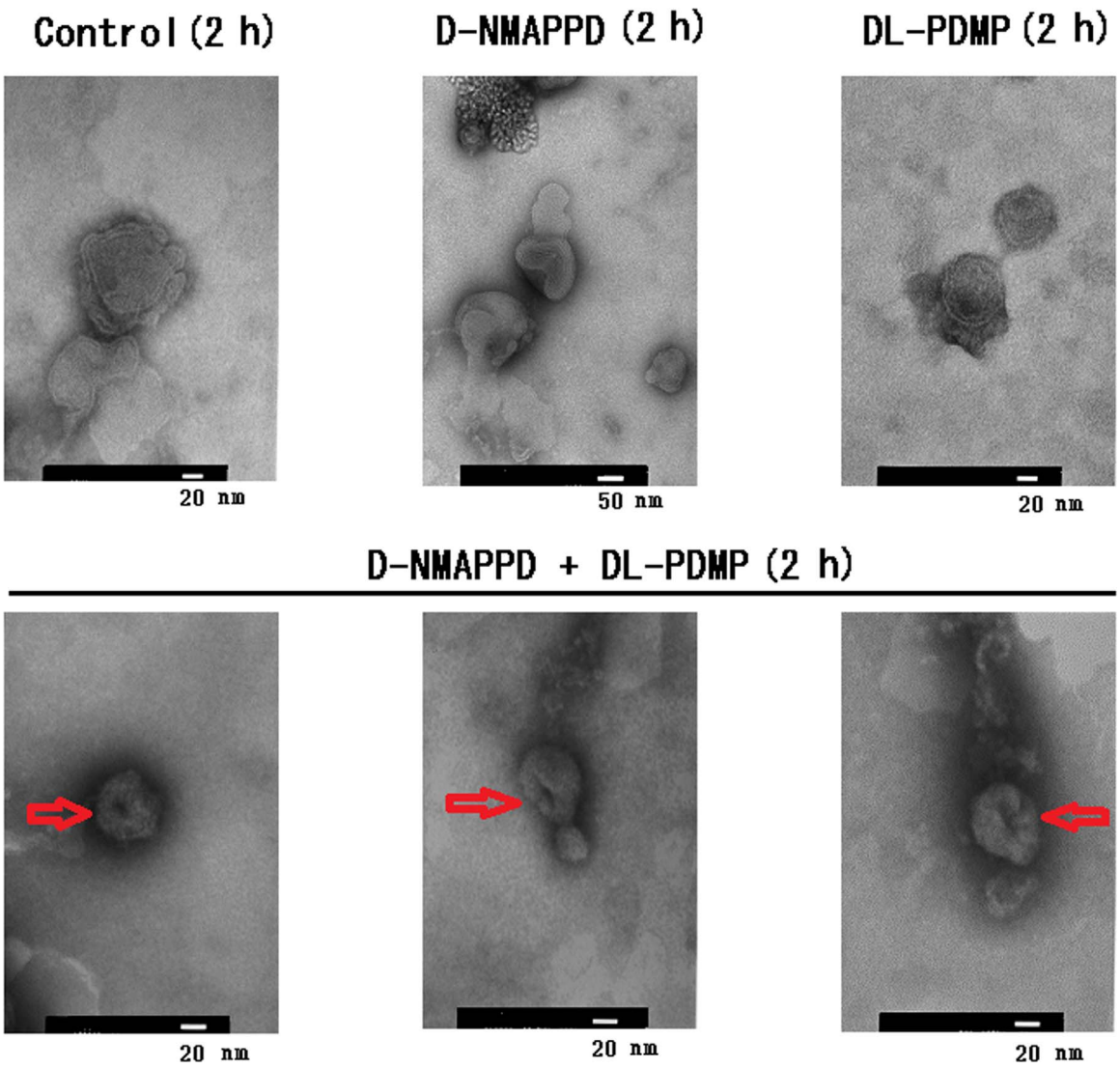

Fig. 3. Transmission electron microscopy of the lysosome-rich fraction after various additions. The lysosome-rich fraction was negatively stained with sodium phosphotungstate, as described in Section 2.

connected reversed-phase HPLC separation as described previously [7].

The quantitative determination of Cers/dihydro-Cers/d18:0/d18:1 by selected ion monitoring (SIM) using HPLC-APCI-MS was performed as described previously [7].

For the quantitative determination of cholesterol by SIM using HPLC-APCI-MS, the peak area of MH^+-H_2O (*m/z* 369) ions as the major base ions from cholesterol was compared with the peak area of MH^+-H_2O (*m/z* 371) ions as the major base ions from β-cholestanol as the IS.

2.8. Transmission electron microscopy of the lysosome-rich fraction

One drop of a suspension with 0.85% sodium chloride from the lysosome-rich fraction was placed on a grid (carbon evaporating collodion grid, 400 mesh) impregnated with water and the excess solvent was wiped with a filter paper. For negative staining, one drop of 2% sodium phosphotungstate was placed on the same plane of the grid and the excess stain was wiped with a filter paper. After air drying of the grid at room temperature, transmission electron microscopic analysis was performed with JEM-1200EXII (JEOL, Japan) at magnifications ranging from the accelerating voltage, 80 kV.

2.9. Morphologic assessment of cells undergoing necrotic cell death and apoptosis

A549 cells were grown in DMEM medium using BD Falcon culture slides with 4 chambers (Bedford, MA, USA). Each chamber was filled with 1.0 mL of DMEM medium containing 3 μL of dimethyl sulfoxide (DMSO) as a control, 1.0 mL of DMEM medium containing 200 μM DL-PDMP/65 μM D-NMAPPD (with 3 μL of DMSO) as the dual addition, 1.0 mL of DMEM medium containing 200 μM DL-PDMP/65 μM D-NMAPPD/5000 μM NAC (with 3 μL of DMSO) as the effect of NAC to the dual addition, or 1.0 mL of DMEM medium containing 200 μM DL-PDMP/65 μM D-NMAPPD/20 μM CA-074Me (with 3 μL of DMSO) as the effect of CA-074Me to the dual addition. Cells were incubated for 4 h, and the adherent cells were washed twice with PBS and stained using the GFP-Certified Apoptosis/Necrosis Detection kit (Enzo Life Sciences, Inc., Farmingdale, NY) plus Vectashield mounting medium with 4',6-diamidino-2-phenylindole (DAPI) to stain the nucleus (Vector Laboratories, Inc., Burlingame, CA). The morphology of the Apoptosis/Necrosis Detection kit-stained A549 cells was examined by confocal laser scanning microscopy using a Zeiss LSM-700 (Carl Zeiss Microscopy GmbH, Jena, Germany). With the Apoptosis/Necrosis Detection kit, early apoptotic cells are stained positive with the apoptosis detection reagent (Annexin V-EnzoGold, Ex/Em: 550/

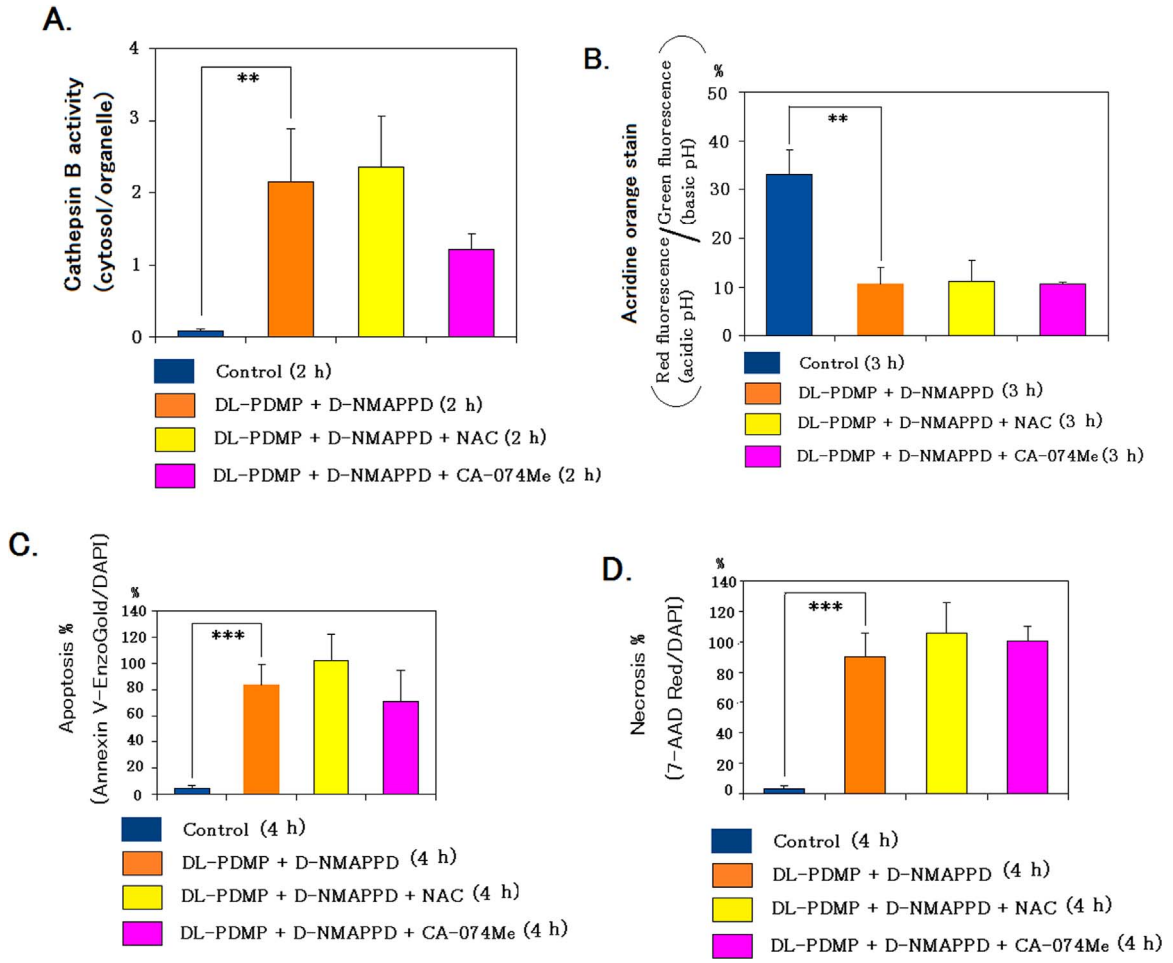

Fig. 4. The individual addition of NAC or CA-074Me to the dual addition of DL-PDMP and D-NMAPPD did not significatly modify cathepsin B activity/acridine orange stain/apoptosis %/necrosis % compared with the dual addition. Cathepsin B activity/acridine orange stain/apoptosis %/necrosis % were achieved as described in Methods. **A-D,** cathepsin B activity/acridine orange stain/apoptosis %/necrosis % in the control or dual/triple addition. Data are presented as the mean values ± S.D. of three independent experiments; **P < 0.01 and ***P < 0.001 as compared with the control.

570 nm, yellow fluorescence) but negative with the necrotic detection reagent. On the other hand, early necrotic cells are stained positive with the necrotic detection reagent (7-AAD, Ex/Em: 546/647 nm, red fluorescence) but negative with the apoptosis detection reagent.

2.10. Lysosomal stability assay

A549 cells were grown using BD Falcon culture slides with 4 chambers, as described above. After the cells were incubated for 2 h, acridine orange was added to a final concentration of 6.6 μM. After the cells were incubated for 45 min, the adherent cells were washed three times with PBS. The morphology of the acridine orange-stained A549 cells was examined by confocal laser scanning microscopy using a Zeiss LSM-700. Acridine orange in active lysosomes with an acidic pH exhibited red fluorescence. On the other hand, acridine orange in the cytoplasm or nucleus with a basic pH exhibited green fluorescence. At the previous stage of plasma membrane disruption, the rupture of acridine orange-loaded lysosomes may be monitored as an increase in cytoplasmic diffuse green fluorescence or a decrease in granular red fluorescence [8].

To measure cathepsin B activity in the cytosol and organelles in A549 cells, cells were incubated for 2 h and fractionated using the Fraction PREP Cell Fractionation kit (BioVision, Milpitas, CA). The cytosolic fraction was fractionated using Cytosol Extraction Buffer containing DTT, and the pellet (organelle fraction) resulting from this fractionation was collected. For the liberation of cathepsin B from the organelle fraction, the pellet was treated with ultrasonic waves for 20 s in 0.85% sodium chloride, and the homogenate was fractionated by centrifugation at 700 × *g* for 10 min. Cathepsin B activity was measured in both the cytosolic and organelle fractions using the Cathepsin B Activity Fluorometric Assay kit (BioVision).

2.11. Statistical analysis

Data are expressed as the mean ± SD of three independent experiments. To determine significance, the values were compared using the two-group *t*-test, with differences considered significant at $P < 0.05$.

3. Results

3.1. The analysis of LAMP-2, Bax and β-actin in the homogenate or lysosome rich fraction from A549 cells by Western blotting

LAMP-2 protein as an indication of lysosomal membrane was concentrated in the lysosome-rich fraction as shown in Fig. 1. However, Bax protein was not detected in the lysosome-rich fraction, as shown in Fig. 1. That is to say, the translation of Bax protein to lysosomes from the cytosol was not caused by the dual addition of DL-PDMP/D-NMAPPD, individual additions, or the control.

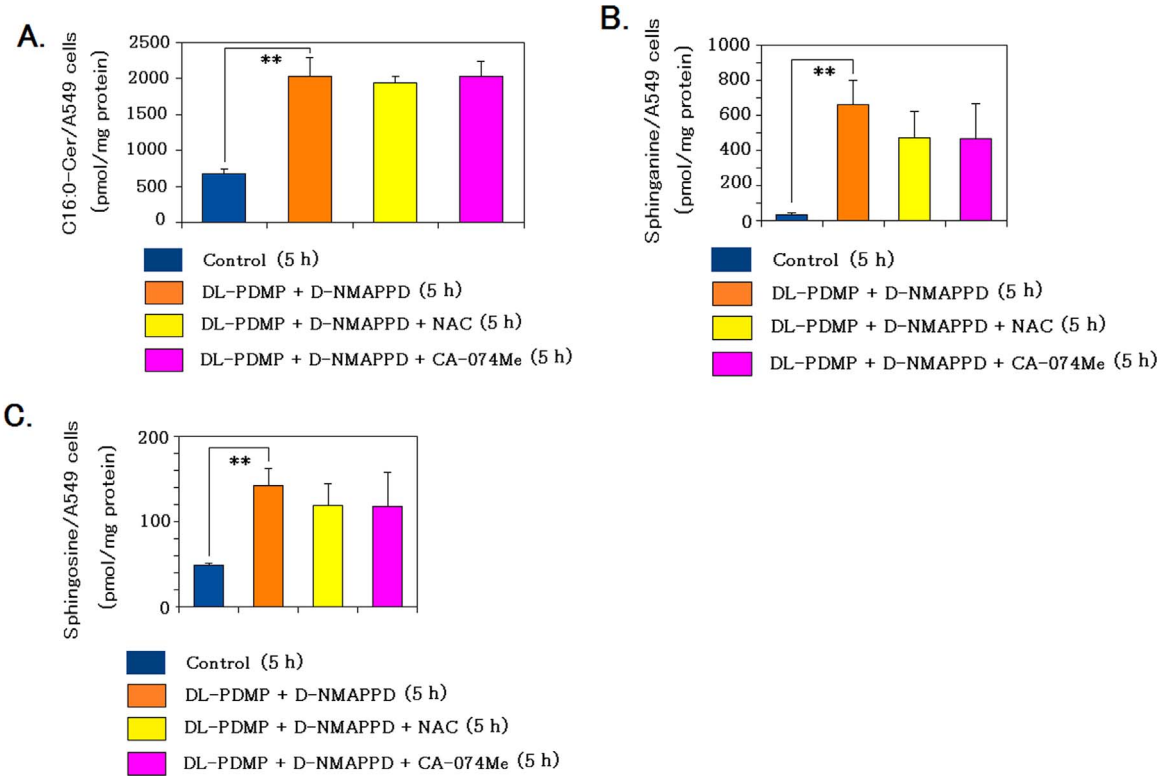

Fig. 5. The individual addition of NAC or CA-074Me to the dual addition of DL-PDMP and D-NMAPPD did not significatly modify C16:0-Cer/sphinganine/sphingosine contents compared with the dual addition. The induction of Cer accumulation and extraction/analysis of C16:0-Cer/sphinganine/sphingosine in the homogenate of A549 cells were achieved as described in Methods. **A–C**, levels of C16:0-Cer/sphinganine/sphingosine in A549 cells 5 h after the control or dual/triple addition. Data are presented as the mean values ± S.D. of three independent experiments; **P < 0.01 as compared with the control.

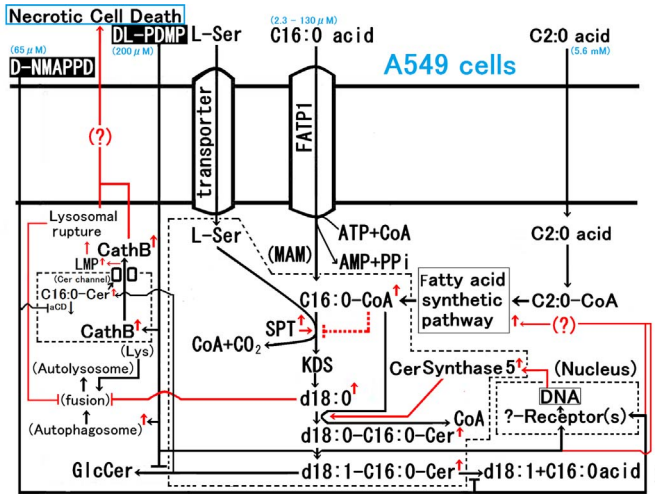

Fig. 6. The dual addition of DL-PDMP and D-NMAPPD to A549 cell culture induced the possibility of Cer channel formation via endogenous C16:0-Cer accumulation in the lysosome membrane as an initial step prior to initiation of necrotic cell death. The findings described in this study are summarized with the findings of Ref. [7]. As for the morphology, the dual addition of DL-PDMP/D-NMAPPD led to black circular structures of 10–20 nm, interpreted as stain-filled cylindrical channels on transmission electron microscopy of the lysosome-rich fraction.

3.2. Contents of Cer species/cholesterol in A549 cells or the lysosome-rich fraction after various additions

The levels of Cer species/dihydro-Cer species in A549 cells or the lysosome-rich fraction 2 h after the individual or dual addition are shown in Fig. 2A–D. The dual addition of DL-PDMP/D-NMAPPD and the individual addition of DL-PDMP caused an increase in C16:0-Cer or dihydro-C16:0-Cer contents compared with the control or individual addition of D-NMAPPD. C16:0-Cer contents were at 2–3 times those of dihydro-C16:0-Cer. Furthermore, C16:0-Cer contents in the lysosome-rich fraction on the dual addition were at 2 times compared with the contents in the homogenate.

The levels of cholesterol in the lysosome-rich fraction 2 h after the individual or dual addition are shown in Fig. 2E. The dual addition of DL-PDMP/D-NMAPPD caused an increase in cholesterol contents in the homogenate and the lysosome-rich fraction compared with the control.

3.3. Transmission electron microscopy of the lysosome-rich fraction after various additions

The lysosome-rich fraction negatively stained with sodium phosphotungstate underwent transmission electron microscopy, as shown in Fig. 3. The dual addition of DL-PDMP/D-NMAPPD led to black circular structures of 10–20 nm, interpreted as stain-filled cylindrical channels, compared with the control and individual addition.

3.4. The effect of adding NACs or CA-074Me to the dual addition on free cathepsin B activity/acridine orange-stain/apoptosis/necrosis in A549 cells

The addition of NAC as an inhibitor of oxidative stress or CA-074Me as an inhibitor of cathepsin B activity to the dual addition did not significantly modify free cathepsin B activity/acridine orange-stain/apoptosis/necrosis in A549 cells (Fig. 4A–D). It is suggested that necrotic cell death in the dual addition was not caused by oxidative stress or cathepsin B activity.

3.5. The effect of adding NACs or CA-074Me to the dual addition on C16:0-Cer/sphinganine/sphingosine contents in A549 cells

The addition of NAC as an inhibitor of oxidative stress or CA-074Me as an inhibitor of cathepsin B activity to the dual addition did not

significantly modify C16:0-Cer/sphinganine/sphingosine contents in A549 cells (Fig. 5A–C). It is suggested that significant increases in C16:0-Cer/sphinganine/sphingosine contents in the dual addition were not caused by oxidative stress or cathepsin B activity.

4. Discussion

We showed that the dual addition of DL-PDMP and D-NMAPPD to A549 cell culture led to the possibility of Cer channel formation via endogenous C16:0-Cer accumulation in the lysosome membrane as an initial step prior to initiation of necrotic cell death. The findings described above and the findings in reference [7] are summarized in Fig. 6. Although the C16:0-Cer channel was inhibited by dihydro-C16:0-Cer or very long-chain Cer (C24:0/C24:1-Cer), as described previously [9,10], the C16:0-Cer contents in dual addition were at 2–3 times those of dihydro-C16:0-Cer or C24:0/C24:1-Cer as shown in Fig. 2A–D. Furthermore, the dual addition of DL-PDMP/D-NMAPPD caused an increase in cholesterol contents in the lysosome-rich fraction compared with the control, as shown in Fig. 2E. Cholesterol was essential for the formation of Cer-channels in the liposomes [11], and a direct cholesterol-Cer interaction in the membrane was considered [12]. On the other hand, the dual addition of DL-PDMP/D-NMAPPD led to black circular structures of 10–20 nm, interpreted as stain-filled cylindrical channels on transmission electron microscopy of the lysosome-rich fraction as the Cer-treated liposomes described previously [11] and shown in Fig. 3. Therefore, the dual addition is causing Cer channel formation via endogenous C16:0-Cer accumulation in the lysosome membrane as an initial step prior to initiation of necrotic cell death. Since the dual addition induced additional endogenous C16:0-Cer accumulation with CerS5 expression and necrotic cell death with lysosomal rupture along with the leakage of cathepsin B/alkalization [7], the formation of C16:0-Cer channels in the lysosome membrane via the inhibition of lysosomal acid ceramidase by D-NMAPPD causes the liberation of cathepsin B from lysosomes for necrotic cell death via C16:0-Cer channels in the lysosome membrane. It is stipulated that the mechanism of C16:0-Cer accumulation in the lysosome with the dual addition is as follows, (a) the rise of CerS 5 activity via an increase of CerS 5 protein expression in the mitochondria associated membrane with the endoplasmic reticulum [6,7], (b) an inhibition of GlcCer synthase in the trans-Golgi network [6,7,13] by DL-PDMP, (c) an inhibition of lysosomal acid ceramidase in the lysosome/late endosome [7,13] by D-NMAPPD.

Activated pro-apoptotic protein Bax is able to permeabilize mitochondria without the need of Cer. Furthermore, treating isolated mitochondria with both activated Bax and Cer induced a higher level of permeabilization than either treatment alone, in synergy [1–3,14–16]. On the other hand, Bax translocates and internalizes into lysosomal membranes [17]. However, since the translation of Bax protein to lysosomes from the cytosol was not caused by the dual addition of DL-PDMP/D-NMAPPD, as shown in Fig. 1, necrotic cell death in the dual addition was free from the contribution of the translation of Bax protein.

Although the effect of ROS (oxidative stress) or cathepsin B as an inducer of lysosomal membrane permeability (LMP) is known [18,19], the addition of NAC [20] as an inhibitor of oxidative stress or CA-074Me [21] as an inhibitor of cathepsin B activity to the dual addition did not significantly modify cathepsin B activity/acridine orange-stain/apoptosis/necrosis in A549 cells (Fig. 4A–D). It is suggested that necrotic cell death in the dual addition was not caused by oxidative stress or cathepsin B activity.

In recent years, tamoxifen-induction of cell death and LMP/C16:0-Cer accumulation with inhibition of Cer hydrolysis (acid ceramidase)/Cer glycosylation in human cells have been reported [22–24]. Since biological effects on the dual addition in this study are similar to the effects of tamoxifen, the function of C16:0-Cer in the cell death was interesting.

5. Conclusions

As an initial step prior to initiation of necrotic cell death, the dual addition of DL-PDMP and D-NMAPPD to A549 cell culture causes Cer channel formation via endogenous C16:0-Cer accumulation in the lysosome membrane with black circular structures interpreted as stain-filled cylindrical channels on transmission electron microscopy. Since the dual addition induced additional endogenous C16:0-Cer accumulation with CerS5 expression and necrotic cell death with lysosomal rupture along with the leakage of cathepsin B/alkalization [7], the formation of C16:0-Cer channels in the lysosome membrane via the inhibition of lysosomal acid ceramidase by D-NMAPPD causes the liberation of cathepsin B from lysosomes for necrotic cell death via C16:0-Cer channels in the lysosome membrane distinct from the mitochondrial caspase-dependent pathway of apoptosis. On the other hand, necrotic cell death in the dual addition was not caused by oxidative stress or cathepsin B activity, and the cell death was free from the contribution of the translation of Bax protein to the lysosome membrane.

References

[1] M. Colombini, Membrane channels formed by ceramide, Handb. Exp. Pharmacol. 215 (2013) 109–126.

[2] M. Abou-Ghali, J. Stiban, Regulation of ceramide channel formation and disassembly: insights on the initiation of apoptosis, Saudi J. Biol. Sci. 22 (2015) 760–772.

[3] M. Colombini, Ceramide channels and mitochondrial outer membrane permeability, J. Bioenerg. Biomembr. (2016), http://dx.doi.org/10.1007/s10863-016-9646-z.

[4] R.D. Sentelle, C.E. Senkal, W. Jiang, S. Ponnusamy, S. Gencer, S.P. Selvam, V.K. Ramshesh, Y.K. Peterson, J.J. Lemasters, Z.M. Szulc, J. Bielawski, B. Ogretman, Ceramide targets autophagosomes to mitochondria and induces lethal mitophagy, Nat. Chem. Biol. 8 (12) (2012) 831–838.

[5] A. Ogura, Y. Watanabe, D. Iizuka, H. Yasui, M. Amitani, S. Kobayashi, M. Kuwabara, O. Inanami, Radiation-induced apoptosis of tumor cells is facilitated by inhibition of the interaction between Survivin and Smac/DIABLO, Cancer Lett. 259 (1) (2008) 71–81.

[6] M. Yamane, K. Miyazawa, S. Moriya, A. Abe, S. Yamane, D,L-Threo-1-phenyl-2-decanoylamino-3-morpholino-1-propanol (DL-PDMP) increases endoplasmic reticulum stress, autophagy and apoptosis accompanying ceramide accumulation via ceramide synthase 5 protein expression in A549 cells, Biochimie 93 (9) (2011) 1446–1459.

[7] M. Yamane, Palmitoyl-ceramide accumulation with necrotic cell death in A549 cells, followed by a steep increase in sphinganine content, Biochim. Open 1 (2015) 11–27.

[8] K. Kagedal, M. Zhao, I. Svensson, U.T. Brunk, Sphingosine-induced apoptosis is dependent on lysosomal proteases, Biochem. J. 359 (Pt 2) (2001) 335–343.

[9] J. Stiban, D. Fistere, M. Colombini, Dihydroceramide hinders ceramide channel formation: implications on apoptosis, Aopotosis 11 (2006) 773–780.

[10] J. Stiban, M. Perera, Very long chain ceramides interfere with C16-ceramide-induced channel formation: a plausible mechanism for regulating the initiation of intrinsic aopotosis, Biochim. Biophys. Acta 1848 (2) (2015) 561–567.

[11] S. Samanta, J. Stiban, T.K. Maugel, M. Colombini, Visualization of ceramide channels by transmission electron microscopy, Biochim. Biophys. Acta 1808 (4) (2011) 1196–1201.

[12] A.B. Garcia-Arribas, A. Alonso, F.M. Goni, Cholesterol interactions with ceramide and sphingomyelin, Chem. Phys. Lipids 199 (2016) 26–34.

[13] M. Goldschmidt Arzi, E. Shimoni, H. Sabanay, A.H. Futerman, L. Addadi, Intracellular localization of organized lipid domains of C16-ceramide/cholesterol, J. Struct. Biol. 175 (1) (2011) 21–30.

[14] V. Ganesan, M.N. Perera, D. Colombini, D. Datskovskiy, K. Chadha, M. Colombini, Ceramide and activated Bax act synergistically to permeabilize the mitochondrial outer membrane, Apoptosis 15 (5) (2010) 553–562.

[15] M.N. Perera, S.H. Lin, Y.K. Peterson, A. Bielawska, Z.M. Szulc, R. Bittman, M. Colombini, Bax and Bcl-xL exert their regulation on different sites of the ceramide channel, Biochem. J. 445 (1) (2012) 81–91.

[16] M.N. Perera, V. Ganesan, L.J. Siskind, Z.M. Szulc, A. Bielawska, R. Bittman, M. Colombini, Ceramide channel: structural basis for selective membrane targeting, Chem. Phys. Lipids 194 (2016) 110–116.

[17] J. Bove, M. Martinez-Vicente, B. Dehay, C. Perier, A. Recasens, A. Bombrun, B. Antonsson, M. Vila, BAX channel activity mediates lysosomal disruption linked to Parkinson disease, Autophagy 10 (5) (2014) 889–900.

[18] A. Terman, T. Kurz, B. Gustafsson, U.T. Brunk, Lysosomal labilization. IUBMB, Life 58 (9) (2006) 531–539.

[19] N.W. Werneburg, M.E. Guicciardi, S.F. Bronk, G.J. Gores, Tumor necrosis factor-alpha-associated lysosomal permeabilization is cathepsin B dependent, Am. J. Physiol. Gastrointest. Liver Physiol. 283 (4) (2002) G947–G956.

[20] A. De, Milito, E. Iessi, M. Logozzi, F. Lozupone, M. Spada, M.L. Marino, et al.,

Proton pump inhibitors induce apoptosis of human B-cell tumors through a caspase-independent mechanism involving reactive oxygen species, Cancer Res. 67 (11) (2007) 5408–5417.

[21] M.C. Michallet, F. Saltel, M. Flacher, J.P. Revillard, I. Genestier, Cathepsin-dependent apoptosis triggered by supraoptimal activation of T lymphocytes: a possible mechanism of high dose tolerance, J. Immunol. 172 (9) (2004) 5405–5414.

[22] S.A. Morad, J.C. Levin, S.F. Tan, T.E. Fox, D.J. Feith, M.C. Cabot, Novel off-target effect of tamoxifen-inhibition of acid ceramidase activity in cancer cells, Biochim. Biophys. Acta 1831 (12) (2013) 1657–1664.

[23] L.A. Kim, D. Amarnani, G. Gnanaguru, W.A. Tseng, D.G. Vavvas, P.A. D'Amore, Tamoxifen toxicity in cultured retinal pigment epithelial cells is mediated by concurrent regulated cell death mechanisms, Investig. Ophthalmol. Vis. Sci. 55 (8) (2014) 4747–4758.

[24] S.A. Morad, S.F. Tan, D.J. Feith, M. Kester, D.F. Claxton, T.P. Loughran Jr, B.M. Barth, T.E. Fox, M.C. Cabot, Modification of sphingolipid metabolism by tamoxifen and N-desmethyltamoxifen in acute myelogenous leukemia-impact on enzyme activity and response to cytotoxics, Biochim. Biophys. Acta 1851 (7) (2015) 919–928.